Revision 1

Effects of thermal annealing on water content and $\delta^{18}O$ in zircon

Word count: 6717

Chuan-Mao Yang[a, b, c], Xiao-Ping Xia[a, b, c*], Yu-Ya Gao[c, d], Xue Wang[e], Wan-Feng Zhang[a, c], Ze-Xian Cui[a, c], Ya-Nan Yang[a, c], Qing Yang[a, c], Yi-Gang Xu[a, b, c]

[a] *State Key Laboratory of Isotope Geochemistry and CAS Center for Excellence in Deep Earth Sciences, Guangzhou Institute of Geochemistry, Chinese Academy of Sciences, Guangzhou 510640, China*

[b] *College of Earth and Planetary Sciences, University of the Chinese Academy of Sciences, Beijing 100049, China*

[c] *Southern Marine Science and Engineering Guangdong Laboratory (Guangzhou) , Guangzhou 511458, China*

[d] *National Institute of Metrology, Beijing 102200, China*

[e] *College of Earth Science and Engineering, Shandong University of Science and Technology, Qingdao 266590, China*

Corresponding author: xpxia@gig.ac.cn

ABSTRACT

Primary water and oxygen isotope composition are important tools in tracing magma source and evolution. Metamictization of zircon due to U-Th radioactive decay may introduce external secondary water to the crystal, thereby masking the primary water and oxygen isotope signature. Recently, Raman-based screening has been established to select the low degree metamict zircons. However, such an approach may not be appropriate to ancient samples, in which nearly all zircons are metamict. It was reported that thermal annealing can potentially heal crystals and retrieve primary water content and $\delta^{18}O$ information from metamict zircons, given the weaker hydrogen bond of secondary water than that of primary water. Heating experiments at temperature of 200–1000°C over a period of 2–10 hours reveal that annealing can effectively recover primary water and oxygen isotopes from metamict zircons. Primary water in crystalline and metamict zircons remains intact when heated at <700°C, whilst secondary water can be effectively expelled from metamict zircons when heated at 600°C for >4 hours, which represent the optimal annealing treatment condition. Hydrothermally-altered zircon is an exception. It only yields the minimum estimate of its primary water contents at 600°C over a period of >4 hours, probably due to partial primary water loss during metamictization for hydrothermal zircons. Moreover, the proportion of low-$\delta^{18}O$ (<4.7‰) zircon grains that may be influenced by secondary water dropped from ~21% at <600°C to ~9% when annealed at >700°C. This study therefore provides the basis for applying zircon water and $\delta^{18}O$ proxies to geologically ancient samples.

Key words: metamict zircon, secondary water, primary water, oxygen isotopes, thermal

annealing, diffusion

INTRODUCTION

Zircon water content and oxygen-hafnium isotope compositions have been widely used as geochemical proxies in constraining igneous processes (Kemp et al., 2007; Liebmann et al., 2021; Meng et al., 2021; Pidgeon et al., 2013, 2017; Valley et al., 1994; Xia et al., 2021; Xu et al., 2021; Yang et al., 2022; Yao et al., 2021). Although zircon is a nominally anhydrous mineral (NAM), it always contains trace amount of water during its crystallization from magma (hereby termed primary water) (De Hoog et al., 2014; Liebmann et al., 2021; Meng et al., 2021; Wang et al., 2018; Xia et al., 2021; Yang et al., 2022; Yao et al., 2021). Water diffuses slowly in zircon (cf. many other NAMs such as garnet and olivine), indicating that zircon can better retain the primary water content (Ingrin and Zhang, 2016; Zhang, 2015). It has reported that primary water was in zircons has the potential to be a sensitive magma hygrometer (Xia et al., 2021). Oxygen isotope composition is a powerful tool to trace source of magma (Valley et al., 1994). For example, Kemp et al. (2007) has identified the crust-mantle mixing origin of I-type granites of eastern Australia from O-Hf isotopes. Acquiring primary water and oxygen isotope composition of zircon can thus reveal melting mechanism and magmatic processes.

Water in crystalline zircon is mainly in the form of OH that is introduced by the hydrogrossular substitution, and charge balance with other cations, such as REEs (Aines and Rossman, 1986; De Hoog et al., 2014; Hoskin and Schaltegger, 2003; Nasdala et al., 2001a;

Trail et al., 2011; Woodhead et al., 1991b; Zhang et al., 2010). However, the U-Th radioactive decay in zircon would cause lattice damage and metamictization (Chakoumakos et al., 1987; Nasdala et al., 1995, 2001b; Palenik et al., 2003; Woodhead et al., 1991a). Crystal lattice of metamict zircon is expanded and open to infiltration of external secondary water (Nasdala et al., 2001a; Pidgeon et al., 2013), thereby masking the primary water content. For example, water content in metamict zircon can be up to 16.3 wt.% (Aines and Rossman, 1986). In metamict zircons, water is present in the form of hydrous mineral inclusions or fluid inclusions (Woodhead et al., 1991). In addition, some neutral H_2O molecules may be present along cracks and grain boundaries (Woodhead et al., 1991). Since the oxygen isotope composition of secondary water may be different from that of zircon, the measured $\delta^{18}O$ of metamict zircons could deviate significantly from its original signature (Gao et al., 2014; Liebmann et al., 2021; Wang et al., 2014; Yang et al., 2022). In addition, zircon with high radiation damage has a different matrix effect from that of crystalline zircon (Allen and Campbell, 2012; Gao et al., 2014; Pidgeon, 2014; White and Ireland, 2012), causing more difficulties to calibrate instrument mass fractionation (Allen and Campbell, 2012; Gao et al., 2014; White and Ireland, 2012).

Uneven distributions of U and Th in zircons result in different degrees of metamictization, occasionally forming metamict and non-metamict zones in a single zircon grain (Nasdala et al., 1996). The most intuitive way to avoid metamictization effect is to select non-metamict zircon grains, for instance by using in-situ Raman to determine the degree of metamictization (Ewing et al., 2003; Nasdala et al., 1995; Nasdala et al., 2001b,

2003; Palenik et al., 2003; Schmidt and Nasdala, 2020; Yang et al., 2022). Crystalline zircons commonly have sharp peaks and strong characteristic vibration peaks of Si-O tetrahedrons, e.g., $\nu_3(SiO_4)$ (Nasdala et al., 1995, 2001b). Raman peaks of metamict grains are relatively smooth with a decreases in peak intensity and a shift of $\nu_3(SiO_4)$ position to a lower wavenumber (Nasdala et al., 1995, 2001b). Based on the full width at half maximum (FWHM) and Raman shift of $\nu_3(SiO_4)$, Yang et al. (2022) developed a screening method for the moderately metamict zircon.

This screening method, however, may not be effective for geologically ancient (e.g., Archean-Proterozoic) samples, in which most zircons are strongly metamict. It is therefore pivotal and timely urgent to establish an approach enabling the geochemical proxies of zircon water and $\delta^{18}O$ for ancient metamict zircons. One way is to thermally anneal zircon, because the O-H···O hydrogen bond of secondary water in metamict zircons is likely longer and weaker than that in pristine grains (due to the larger unit cell volume of metamict zircons) (Nasdala et al., 2001a). Compared with crystalline zircon, water in metamict zircon would be expelled at a lower temperature (Nasdala et al., 2001a). Meanwhile, the damaged metamict zircon lattice can be thermally-annealed and hence the matrix effect in Secondary Ion Mass Spectrometry (SIMS) isotope analysis eliminated (Allen and Campbell, 2012; Pidgeon, 2014; Zhang et al., 2003).

Previous studies yielded different behaviors of water in zircon during annealing (Aines and Rossman, 1986; Caruba et al., 1985; Nasdala et al., 2001a; Woodhead et al., 1991b). Thermogravimetric curves revealed that zircon, whether crystalline or metamict, begins to

dehydrate at a temperature even as low as 50°C (Caruba et al., 1985; Nasdala et al., 2001a), and the water is largely expelled when the zircon is heated to a temperature of ~600°C. In contrast, infrared (IR) spectra of heat-treated zircon revealed that water content in moderately metamict zircon rarely drop at/below 530°C (Nasdala et al., 2001a; Woodhead et al., 1991b). Clearly more thermal annealing experiments are needed to assess the optimal annealing conditions (incl. heating temperature and time duration) to minimize the metamictization effect on SIMS water content and oxygen isotope analyses. In this article, zircon samples with different degrees of metamictization were selected for the thermal annealing experiment, with the aims to investigate (i) whether secondary water is present in metamict zircon, and (ii) under what heating conditions can the secondary water be expelled completely.

SAMPLE DESCRIPTIONS

Zircon samples selected for the experiment are: (1) crystalline Penglai zircon megacryst (Li et al., 2010), (2) Suzhou A-type granite zircon with varying degrees of metamictization (Sz2, partially metamict) (Gao et al., 2014; Yang et al., 2022), and (3) Archean TTG gneiss zircon with nearly all zircons metamict (THX13120, fully metamict) (Cui et al., 2022). Metamictization degrees of THX13120 are lower than that of zircons in Sz2 with the highest metamictization degrees (Cui et al., 2022; Gao et al., 2014; Yang et al., 2022). Penglai zircon megacrysts from early Pliocene alkaline basalt (Hainan Island, South China) are in-house standards for oxygen and hafnium isotope analyses (Li et al., 2010). They have homogeneous oxygen isotope composition with the recommended $\delta^{18}O$ value of 5.31 ± 0.10‰ (2SD) (Li et

al., 2010). The Penglai zircon has low water content (20–200 ppm; Yang et al., 2022). The Penglai zircon megacrysts were crushed into ~100 μm fragments. The Sz2 zircon is from the Early Cretaceous A-type granites near Suzhou city (Jiangsu, South China), and contains varying U (33–13,433 ppm, commonly high-U) and Th (13–17,028 ppm) contents (Gao et al., 2014). The degree of zircon metamictization varies greatly from crystalline to highly-metamict, as revealed by Raman spectrum (Gao et al., 2014; Yang et al., 2022). The oxygen isotope ($\delta^{18}O$ = 3.5–6.5‰) and water content (600 to >5000 ppm) of Sz2 zircon are variable (Gao et al., 2014; Yang et al., 2022). The low-$\delta^{18}O$ zircons are associated with high water content, probably due to the larger amount of meteoric water in the crystalline zircon lattice (Gao et al., 2014; Yang et al., 2022). THX13120 zircon is from a TTG gneiss (U-Pb age: 2.19 Ga) in the Paleoproterozoic Taihua Group, North China Craton (Cui et al., 2022; Diwu et al., 2014). The zircon is highly-metamict and the water content varies from 700 to 2100 ppm (median 1458 ppm) (Cui et al., 2022). Most Sz2 and THX13120 zircon grains are >100 μm long (Fig. 1).

<Figure 1>

ANALYTICAL METHODS

Thermal annealing

Zircon grains or fragments from the three samples were randomly assigned into different zircon fractions, placed inside quartz crucibles, and then heated for 2 h in a muffle furnace to 200°C, 300°C, 400°C, 500°C, 600°C, 700°C, 800°C, 900°C, 1000°C under one atmospheric

pressure (1 atm). The experiment was conducted at the Guangzhou Institute of Geochemistry, Chinese Academy of Sciences (GIGCAS), with a thermocouple installed in the muffle furnace for temperature measurement (±3°C fluctuation). The heating rate was 15°C/min. After heating, the annealed zircon samples cooled quickly (<10 min) to a room temperature. To assess the effect of heating time duration, different zircon fractions were heated at 600°C for 4, 6, 8 and 10 hours. Consequently, a total of 39 thermally-annealed zircon samples were obtained.

SIMS zircon water and oxygen isotope analyses

All samples and zircon standards were mounted on the slide with double-sided adhesive tapes. Zircon SA01 (6.2‰) or Qinghu (5.4‰) was used as the external standard for oxygen isotope calibration (Huang et al., 2019; Li et al., 2013). The samples were then encapsulated in a tin alloy mount, and polished to expose the zircon interior (Zhang et al., 2018). The samples were then observed with cathodoluminescence (CL) imaging and reflected-light petrography to select the analysis spots that are free of cracks or inclusions (Fig. 1).

The zircon oxygen isotope and water contents were measured simultaneously with a CAMECA IMS 1280-HR SIMS at the GIGCAS. The zircon water content was obtained by the relationship between water contents and the measured $^{16}O^{1}H/^{16}O$ of several in-house reference materials (ZG3, ZG6, ZG7, D16314-2, D15395-3, D15395-4, GJ-1, 91500) (Xia et al., 2019). The analytical uncertainty of water content is ~10% (Xia et al., 2019). The $^{18}O/^{16}O$ value was normalized to the Vienna Standard Mean Ocean Water (VSMOW), whose $^{18}O/^{16}O$

= 0.0020052. Details of the method are as described by Xia et al. (2019). The analysis chamber was cooled by liquid nitrogen to maintain a high vacuum of ~1.9×10^{-9} mbar, in which the detection limit of water is ~10 ppm. The widths of the quadratic sputtered area and analytical area are 50 μm and 30 μm (15 μm spot size + 15 μm rastering), respectively. The ^{16}O and ^{18}O signals were configured with 500 μm collector slits to generate mass resolution power (MRP) of ~2500. To avoid ^{17}O interference, a 173 μm collection slit, corresponding to ~7000 MRP, was used for $^{16}O^{1}H$. The internal $^{18}O/^{16}O$ and $^{16}O^{1}H/^{16}O$ precisions are usually better than 0.4% and 0.5% (2SE), respectively.

Laser Raman spectroscopy

The analysis was performed with a Renishaw 2000 Raman spectrometer at the GIGCAS. The laser Raman spectral light source is a 532 nm argon laser. The telephoto objective lens has a 20X magnification, using 3×3 μm spot size. The Raman signal generated by the samples is split by a grating with 2400 grooves per millimeter, and then collected by a thermoelectric cooled charge coupled device (CCD). The average spectral resolution is ~1 cm^{-1}. The time duration of spectral collection varies with the signal intensity (10–200 s). 100–1400 cm^{-1} full-wavelength spectrum was taken at one time, and the single crystal silicon wafer was used to calibrate the Raman spectra before the measurement. The Raman shift of the single crystal silicon wafer was corrected to 520.7 cm^{-1}.

RESULTS

This is the peer-reviewed, final accepted version for American Mineralogist, published by the Mineralogical Society of America.
The published version is subject to change. Cite as Authors (Year) Title. American Mineralogist, in press.
DOI: https://doi.org/10.2138/am-2022-8444. http://www.minsocam.org/

Water content and $\delta^{18}O$ value in zircons annealed at different temperature

To evaluate the heating effect on pristine zircons, the Penglai zircon samples (20–200 ppm water) (Yang et al., 2022) were heated at <600°C, 700°C, 800°C, 900°C, and 1000°C. As shown in Figure 2a, the zircon water content remains constant when heating at <700°C, but drops to one third of its initial content at 700°C, 800°C, 900°C, and rises slightly at 1000°C (Fig. 2a). Water content of the untreated Sz2 zircon is relatively high (median 997 ppm) and variable (650 to >5000 ppm, mostly 750–2000 ppm) (Fig. 2b) (Yang et al., 2022). Significant water loss at ~700–800°C is also observed (Fig. 2b). The median water content in zircons annealed at 600°C is comparable to that of the untreated zircon. However, it is noteworthy that the water content below 400°C rises with temperature, and starts to fall when heated at > 400°C (Fig. 2b). The minimum water content at 500°C (~460 ppm) is lower than that of the untreated zircon (~650 ppm). Slightly increasing water content at 1000°C was also observed (Fig. 2b). Water content in the fully-metamict THX13120 zircon annealed at 200–700°C are similar (750–2000 ppm, median ~1500 ppm), and drops considerably to 505 ppm (median) when annealed at 800°C. The water content is further reduced to 80 ppm (median) at 900°C, approximately one-tenth of the untreated zircon water content (Fig. 2c).

<Figure 2>

Prominent oxygen isotope changes in zircon were only observed for Sz2 zircon samples (Fig. 3): the $\delta^{18}O$ range in zircons heated at >700°C is much narrower than that heated <700°C. Median $\delta^{18}O$ values for individual Penglai and TH13120 zircons heated at various

temperatures are all consistent (within error), even when substantial amount of secondary water is expelled from zircons at >700°C (Fig. 3).

<Figure 3>

Water content and $\delta^{18}O$ in zircons annealed at 600°C for different time duration

For the Penglai and THX13120 zircons annealed at 600°C, their water content remains constant irrespective of the heating duration (Fig. 4a, c). The water content range and median value of Sz2 zircon remain relatively constant when the time duration is no more than four hours (Fig. 4b). In contrast, the maximum, minimum and median water contents decrease, and the variation range becomes narrower when the zircons were heated for six hours or longer (Fig. 4b). However, the oxygen isotopes of all the three zircon samples are virtually unaffected by the heating duration (Fig. 5).

<Figure 4>

<Figure 5>

Raman spectra of annealed zircons

The Penglai zircons always display intrinsic sharp Raman peaks when heated at 200–1000°C, indicating no crystal structure transformation of crystalline zircon. In contrast, Raman spectra of Sz2 zircon samples show both sharp and very flat Raman spectra for the untreated grains and those annealed at <400°C (Fig. 6a). The spectra become sharper (the number of smooth-spectra zircon falls drastically) when the temperature increased to 800°C

This is the peer-reviewed, final accepted version for American Mineralogist, published by the Mineralogical Society of America.
The published version is subject to change. Cite as Authors (Year) Title. American Mineralogist, in press.
DOI: https://doi.org/10.2138/am-2022-8444. http://www.minsocam.org/

and 1000℃ (Fig. 6a). All the unannealed THX13120 zircon grains are characterized by broad spectra and wide $\nu_3(SiO_4)$ (FWHM >8 cm^{-1}; Fig. 6b). Albeit the larger fraction of metamict zircons in THX13120 than in Sz2, the metamictization degree of THX13120 is generally lower than Sz2, as indicated by their smoother Raman spectra and $\nu_3(SiO_4)$ width (Fig. 6). Up to 600℃, only few zircon grains have crystalline zircon spectra, whilst most THX13120 zircon grains were transformed into crystalline at 1000℃ (Fig. 6b).

<Figure 6>

DISCUSSION

Primary and secondary water in crystalline and metamict zircons

Secondary water is absent in Penglai zircons because these zircons are completely crystalline, and thus only primary water dehydration occurred during the annealing. As shown in Figure 2a, the diffusion loss of solely primary water started at 700℃, and the water content fell to about half of that for the unannealed grains (Fig. 2a). Primary water in the Penglai zircon samples remains constant at <700℃. Although THX13120 zircon is strongly-metamict and has more water, dehydration only occurred when it was heated at ~800℃ (Fig. 2c). The similar water behavior between the Penglai and THX13120 samples implies the presence of only primary water (i.e., no secondary water) in THX13120. This is because although metamictization can produce space for secondary water storage (Nasdala et al., 2001a), secondary water would not necessarily enter these spaces (Nasdala et al., 2001a; Yang et al., 2022). This is further supported by the phenomenon that secondary water dehydration was

not observed during the annealing (Figs. 2, 3). Thus, primary water in metamict zircon is as stable as in crystalline zircon, and some old, strongly-metamict zircons can still retain their primary water content.

Previous studies have documented that the Taihua Group underwent upper amphibolite to granulite facies metamorphism with the peak metamorphic age of ~1.92 Ga (Lu et al., 2017; Zhai et al., 2005). The pseudosection modelling suggests metamorphic temperature may reach >800°C (Lu et al., 2017). As a result, the primary water content may have been reset during metamorphism. However, TTG samples with similar compositions and metamorphic degrees but different tectonic settings in Taihua Group have distinct zircon water contents, implying primary water in zircon are not disturbed (Cui et al., 2022). This is either because metamorphic temperature is not as high as predicted by modelling, or the onset temperature for primary water loss is higher at the metamorphic condition than that for our experiment due to the higher pressure.

Like Penglai and THX13120 zircons, intensive dehydration was observed in Sz2 which contains both metamict and crystalline zircons (Figs. 2, 4) when heated at 700–800°C, yet moderate dehydration also occurred in Sz2 at <600°C (Fig. 2b). The Sz2 water content significantly dropped when heated at 600°C for over four hours (Fig. 4b). Probably, this may have result from the escape of secondary water, since primary water in both crystalline and metamict zircons are stable under such low temperature. It is interesting that the onset temperature of primary water loss in the crystalline Penglai zircons (~700°C) is lower than that of metamict THX13120 and Sz2 zircons (~800°C) (Fig. 2). The temperature difference is

attributed to lower content of REE in Penglai zircon grains, which may decrease the chemical bonding of water. Furthermore, lower water contents in Penglai zircons make its loss at a lower temperature more noticeable (Cui et al., 2022; Yang et al., 2022).

Both secondary and primary water are present in Sz2, but only primary water is present in THX13120. This brings the question of whether (and if so, how) one can assess the presence of secondary water in a given sample. In Sz2, water and $\delta^{18}O$ contents are highly variable and high water content is associated with low $\delta^{18}O$ (Fig. 7a) (Yang et al., 2022), suggesting a meteoric origin for the secondary water (Gao et al., 2014; Yang et al., 2022). In contrast, the water and $\delta^{18}O$ contents in THX13120 fall into a narrow range with no discernible correlation, again indicative of the lack of secondary water (Fig. 7b). Since water content in zircon is commonly <2000 ppm, the very-high water content (e.g., >5000 ppm) in Sz2 thus suggests secondary water occurrence (Cui et al., 2022; Meng et al., 2021; Xia et al., 2019, 2021; Yang et al., 2022; Yao et al., 2021). Additionally, LREE-enrichment in some Sz2 zircon grains may also be hydrothermal alteration-related (Fig. 7c-d). In contrast, magmatic zircons in THX13120 are all unaltered (Bell et al., 2016; Hoskin, 2005). In brief, markedly-variable water and oxygen isotope contents with negative correlation and hydrothermal-type REE compositions, as well as flat Raman spectra could collectively be regarded as the diagnostics of presence of secondary-water in zircons.

<Figure 7>

The presence of appreciable amount of water in zircons heated to >800°C deserves

This is the peer-reviewed, final accepted version for American Mineralogist, published by the Mineralogical Society of America.
The published version is subject to change. Cite as Authors (Year) Title. American Mineralogist, in press.
DOI: https://doi.org/10.2138/am-2022-8444. http://www.minsocam.org/

295 explanation (Fig. 2). It was suggested that there may be more stable primary water in zircons
296 (Caruba et al., 1985; Nasdala et al., 2001a; Zhang et al., 2010). When heated at >900°C, all
297 the three samples show a slight water content increase (Fig. 2), which can be attributed to the
298 absorption of atmospheric water by zircon at 1000°C or the uneven distribution of water in
299 zircon.
300
301 **Optimal annealing conditions to obtain reliable primary water content**
302 To obtain reliable primary water content from metamict zircons, it is essential to
303 formulate suitable annealing conditions to remove all secondary water while keeping primary
304 water as much as possible. As discussed above, the primary water begins to escape at 700–
305 800°C, and the water content remains constant at <700°C for both crystalline and metamict
306 zircons. The critical temperature of ~700°C for primary water diffusion is supported by IR
307 analysis of previous stepwise heating experiments (Nasdala et al., 2001a; Woodhead et al.,
308 1991b). Accordingly, a maximum annealing temperature of 600°C was set to retrieve the
309 primary water content (Fig. 4a).
310 Dehydration of primary water is also dependent on the zircon grain size and diffusion
311 direction along the crystal axis (Ingrin and Zhang, 2016; Zhang, 2015). To investigate their
312 effects, a series of modelling was conducted based on the hydrogen diffusion rate in zircon.
313 Recent hydrogen-deuterium (H-D) exchange experiments yielded two different diffusion
314 rates along three axis of zircon (Ingrin and Zhang, 2016; Zhang, 2015). The diffusion rate
315 along axis [001] is higher than those along axis [100] and [010] (Ingrin and Zhang, 2016;

316 Zhang, 2015), which can be expressed as:

317 $D_{[100][010]} = D_0 \exp\left[\frac{-(374\pm39)kJ/mol}{RT}\right],\ logD_0(m^2s^{-1}) = 2.24 \pm 1.57$

318 $D_{[001]} = D_0 \exp\left[\frac{-(334\pm49)kJ/mol}{RT}\right],\ logD_0(m^2s^{-1}) = 1.11 \pm 0.22$

319 where D = diffusion coefficient at different temperature; R and T = ideal gas constants and
320 temperatures, respectively.

321 In this study, the largest diffusion coefficient along the [001] direction was used.
322 One-dimensional diffusion equation was used to simulate the water behavior in zircon,
323 assuming that the water content on the zircon grain margin is 0 ppm (Xu et al., 2019):

$$\frac{c}{c_0}(x,t) = \frac{4}{\pi}\sum_{j=0}^{\infty}\frac{1}{2j+1}sin\frac{(2j+1)\pi x}{h}\cdot\exp\left(-\left[\frac{(2j+1)\pi}{h}\right]^2 Dt\right)$$

324 where c/c_0 is the ratio of the annealed zircon water content c to its initial water content c_0;
325 h is the length of zircon grain in m; D is diffusion coefficient of zircon in m^2s^{-1}; t = diffusion
326 time in s; j is index of summation. The first 300 items on the right side of the equation were
327 used in the calculation.

328 The fractions of preserved water at variable temperatures and positions in 100-μm zircon
329 are illustrated in Figure 8. The water in zircon does not diffuse out until ~700°C, and the
330 diffusion occurs only on the zircon margins (<10 μm from margin) at 700–850°C. At 900–
331 1000°C, zircon can preserve only 0–40% of the original water content with the water in the
332 core largely expelled (Fig. 8). The simulated fractions of preserved water at different
333 temperatures are comparable with our thermal annealing experimental results (Fig. 2).
334 Modelling with smaller zircon grains (40 μm long) for longer duration of heating (6 and 10
335 hours) shows that zircon water content remains stable at 600°C, and minor amount of water

may be diffused out along the zircon margins at 700–800°C.

<Figure 8>

The modelling results suggest that secondary water starts to escape at <600°C. Nevertheless, the median water content in Sz2 (heated at ~600°C for 2h) is not lower than that of unannealed zircon (Fig. 2b), and the water content actually increases when heated at 200–400°C (Fig. 2b). Such a phenomenon was observed also in IR spectrum from stepwise heating experiment, and has been attributed to the movement of hydrogen in a disordered site to an ordered site (Woodhead et al., 1991b). The water content in Sz2 begins to decrease from 400 to 600°C (Fig. 2b), with the lowest water content (~250 ppm) occurred at 500°C, even lower than that of unannealed zircons (~600 ppm; Fig. 2b) (Yang et al., 2022). This suggests that at 500°C, secondary water is unstable and subjected to mild diffusion loss. Therefore, heating of zircons at 600°C for >4 hours likely represent the optimal annealing conditions, which ensure the complete removal of secondary water and retain the maximum amount of primary water (Fig. 4b).

Retrieving primary water content and $\delta^{18}O$ by thermal annealing

It is noteworthy that the water content in Sz2 metamict zircons (annealed at 600°C for >4 hours) is lower than the primary water content estimated from crystalline zircons (screened by Raman spectra) (Fig. 9a) (Yang et al., 2022). This suggests that some primary water in Sz2 metamict zircon was lost either during the annealing or metamictization. Since primary water

in both crystalline or metamict zircons is stable at <700°C (Figs. 2, 4), the primary water loss in Sz2 most likely resulted from geological processes rather than from thermal annealing. The Suzhou alkaline granites were variably hydrothermally altered, which may have affected the zircons and influenced the primary water content (Liebmann et al., 2021; Pidgeon et al., 2017; Wang et al., 2014). The phosphorus content (P ion is an important cation in charge balance with water) in metamict zircons is indeed lower than that of crystalline zircons (Yang et al., 2022), suggesting that the primary water signature is disturbed. Thus, thermal annealing of Sz2 zircon cannot retrieve its primary water content, which has been partly lost in its geological history. In that case, the primary water content obtained from hydrothermally-altered zircon only represents the minimum estimate of its original value (Fig. 9a). In addition, the thermal annealing method is no longer applicable to the case that hydrogen and oxygen isotope exchange occurred intensively between secondary water and zircon. However, intensive oxygen isotope exchange is uncommon for the extremely slow oxygen diffusion rate in zircon (Cherniak and Watson, 2003).

$\delta^{18}O$ remains unchanged at 600°C, >4 hours, which implies the loss of secondary water does not cause oxygen isotopic fractionations between secondary water and zircon. As shown in Figure 9b, higher annealing temperature corresponds to narrower $\delta^{18}O$ range. Proportion of low-$\delta^{18}O$ zircons (<4.7‰) has dropped from ~21% at <600°C for 2 hours to ~9% at >700°C. Therefore, heating metamict zircons above 700°C for a long time can yield more accurate oxygen isotope compositions. The distorted zircon crystal lattice has been fully restored under such high temperature, and the matrix effect (e.g., on zircon U-Pb isotope analysis) is

This is the peer-reviewed, final accepted version for American Mineralogist, published by the Mineralogical Society of America.
The published version is subject to change. Cite as Authors (Year) Title. American Mineralogist, in press.
DOI: https://doi.org/10.2138/am-2022-8444. http://www.minsocam.org/

effectively suppressed (Fig. 6) (Allen and Campbell, 2012), accompanied by both primary and secondary water contents dramatically decrease (Fig. 9a). The more accurate $\delta^{18}O$ measurement of zircons annealed at >700°C likely resulted from the elimination of fractionation of secondary water and matrix effect from the metamict zircons.

<Figure 9>

IMPLICATIONS

From our annealing experiments (200–1000°C for 2 h, and 600°C for 2–10 hours), the following conclusions can be drawn:

(1) Heating at 600°C for >4 hours appear to be the optimal treatment conditions for obtaining primary water content from metamict zircons.

(2) Hydrothermally-altered zircons may have lost some of their primary water during metamictization. Consequently, thermal annealing of these zircons can only yield the minimum estimate of their primary water content.

(3) Thermal annealing at >700°C could improve the oxygen isotope measurement by eliminating secondary water and matrix effect from metamict zircons.

(4) Thermal annealing of zircon has great potential in recovering primary water and oxygen isotope contents from metamict zircons, especially for those from geologically ancient samples.

Acknowledgements

399 This study was supported by the National Natural Science Foundation of China (41688103,
400 41673010), the Key Special Project for Introduced Talents Team of Southern Marine Science
401 and Engineering Guangdong Laboratory (Guangzhou) (GML2019ZD0202) and the Strategic
402 Priority Research Program of the Chinese Academy of Sciences (XDB18000000). We thank
403 Li Ao for helping with the Raman spectroscopic analyses. This is contribution No. IS***
404 from GIGCAS.

405

406 **References Cited**

407 Aines, R.D., and Rossman, G.R. (1986) Relationships between Radiation-Damage and Trace
408 Water in Zircon, Quartz, and Topaz. American Mineralogist, 71(9-10), 1186-1193.
409 Allen, C.M., and Campbell, I.H. (2012) Identification and elimination of a matrix-induced
410 systematic error in LA–ICP–MS 206Pb/238U dating of zircon. Chemical Geology,
411 332-333, 157-165.
412 Bell, E.A., Boehnke, P., and Harrison, T.M. (2016) Recovering the primary geochemistry of
413 Jack Hills zircons through quantitative estimates of chemical alteration. Geochimica
414 et Cosmochimica Acta, 191, 187-202.
415 Caruba, R., Baumer, A., Ganteaume, M., and Iacconi, P. (1985) An Experimental-Study of
416 Hydroxyl-Groups and Water in Synthetic and Natural Zircons - a Model of the
417 Metamict State. American Mineralogist, 70(11-12), 1224-1231.
418 Chakoumakos, B.C., Murakami, T., Lumpkin, G.R., and Ewing, R.C. (1987)
419 Alpha-decay-induced fracturing in zircon: the transition from the crystalline to the

metamict state. Science, 236(4808), 1556-9.

Cherniak, D.J., and Watson, E.B. (2003) Diffusion in Zircon. Reviews in Mineralogy and Geochemistry, 53(1), 113-143.

Cui, Z.-X., Xia, X.-P., Huang, X.-L., Xu, J., Yang, Q., Zhang, W.-F., Zhang, L., Lai, C.-K., and Wang, X. (2022) Meso- to Neoarchean geodynamic transition of the North China Craton indicated by H_2O-in-zircon for TTG suite. Precambrian Research, 371.

De Hoog, J.C.M., Lissenberg, C.J., Brooker, R.A., Hinton, R., Trail, D., Hellebrand, E., and EIMF. (2014) Hydrogen incorporation and charge balance in natural zircon. Geochimica Et Cosmochimica Acta, 141, 472-486.

Diwu, C., Sun, Y., Zhao, Y., and Lai, S. (2014) Early Paleoproterozoic (2.45–2.20Ga) magmatic activity during the period of global magmatic shutdown: Implications for the crustal evolution of the southern North China Craton. Precambrian Research, 255, 627-640.

Ewing, R.C., Meldrum, A., Wang, L.M., Weber, W.J., and Corrales, L.R. (2003) Radiation effects in zircon. Rev Mineral Geochem, 53, 387-425.

Gao, Y.Y., Li, X.H., Griffin, W.L., O'Reilly, S.Y., and Wang, Y.F. (2014) Screening criteria for reliable U–Pb geochronology and oxygen isotope analysis in uranium-rich zircons: A case study from the Suzhou A-type granites, SE China. Lithos, 192-195, 180-191.

Hoskin, P.W.O. (2005) Trace-element composition of hydrothermal zircon and the alteration of Hadean zircon from the Jack Hills, Australia. Geochimica et Cosmochimica Acta, 69(3), 637-648.

Hoskin, P.W.O., and Schaltegger, U. (2003) The composition of zircon and igneous and metamophic petragenesis. Reviews in Mineralogy and Geochemistry, 53(1), 27-62.

Huang, C., Wang, H., Yang, J.H., Ramezani, J., Yang, C., Zhang, S.B., Yang, Y.H., Xia, X.P., Feng, L.J., Lin, J., Wang, T.T., Ma, Q., He, H.Y., Xie, L.W., and Wu, S.T. (2019) SA01 – A Proposed Zircon Reference Material for Microbeam U-Pb Age and Hf-O Isotopic Determination. Geostandards and Geoanalytical Research, 44(1), 103-123.

Ingrin, J., and Zhang, P.P. (2016) Hydrogen diffusion in Zircon. EGU General Assembly Conference Abstracts, 18, p. EPSC2016-7148, Vienna.

Kemp, A.I., Hawkesworth, C.J., Foster, G.L., Paterson, B.A., Woodhead, J.D., Hergt, J.M., Gray, C.M., and Whitehouse, M.J. (2007) Magmatic and crustal differentiation history of granitic rocks from Hf-O isotopes in zircon. Science, 315(5814), 980-3.

Li, X.H., Long, W.G., Li, Q.L., Liu, Y., Zheng, Y.F., Yang, Y.H., Chamberlain, K.R., Wan, D.F., Guo, C.H., Wang, X.C., and Tao, H. (2010) Penglai Zircon Megacrysts: A Potential New Working Reference Material for Microbeam Determination of Hf-O Isotopes and U-Pb Age. Geostandards and Geoanalytical Research, 34(2), 117-134.

Li, X.H., Tang, G.Q., Gong, B., Yang, Y.H., Hou, K.J., Hu, Z.C., Li, Q.L., Liu, Y., and Li, W.X. (2013) Qinghu zircon: A working reference for microbeam analysis of U-Pb age and Hf and O isotopes. Chinese Science Bulletin, 58(36), 4647-4654.

Liebmann, J., Spencer, C.J., Kirkland, C.L., Xia, X.P., and Bourdet, J. (2021) Effect of water on $\delta^{18}O$ in zircon. Chemical Geology, 574.

Lu, J.S., Zhai, M.G., Lu, L.S., Wang, H.Y.C., Chen, H.X., Peng, T., Wu, C.M., and Zhao, T.P.

(2017) Metamorphic P–T–t path retrieved from metapelites in the southeastern Taihua metamorphic complex, and the Paleoproterozoic tectonic evolution of the southern North China Craton. Journal of Asian Earth Sciences, 134, 352-364.

Meng, J.T., Xia, X.P., Ma, L., Jiang, Z.Q., Xu, J., Cui, Z.X., Yang, Q., Zhang, W.F., and Zhang, L. (2021) A H_2O-in-zircon perspective on the heterogeneous water content of crust-derived magmas in southern Tibet. Science China Earth Sciences, 64(7), 1184-1194.

Nasdala, L., Beran, A., Libowitzky, E., and Wolf, D. (2001a) The incorporation of hydroxyl groups and molecular water in natural zircon ($ZrSiO_4$). American Journal of Science, 301(10), 831-857.

Nasdala, L., Irmer, G., and Wolf, D. (1995) The degree of metamictization in zircon: a Raman-spectroscopic study. European Journal of Mineralogy, 7(3), 471-478.

Nasdala, L., Pidgeon, R.T., and Wolf, D. (1996) Heterogeneous metamictization of zircon on a microscale. Geochimica et Cosmochimica Acta, 60(6), 1091-1097.

Nasdala, L., Wenzel, M., Vavra, G., Irmer, G., Wenzel, T., and Kober, B. (2001b) Metamictisation of natural zircon: accumulation versus thermal annealing of radioactivity-induced damage. Contributions to Mineralogy and Petrology, 141(2), 125-144.

Nasdala, L., Zhang, M., Kempe, U., Panczer, G., Gaft, M., Andrut, M., and Plotze, M. (2003) Spectroscopic methods applied to zircon. Reviews in Mineralogy and Geochemistry, 53, 427-467.

Palenik, C.S., Nasdala, L., and Ewing, R.C. (2003) Radiation damage in zircon. American Mineralogist, 88(5-6), 770-781.

Pidgeon, R.T. (2014) Zircon radiation damage ages. Chemical Geology, 367, 13-22.

Pidgeon, R.T., Nemchin, A.A., and Cliff, J. (2013) Interaction of weathering solutions with oxygen and U–Pb isotopic systems of radiation-damaged zircon from an Archean granite, Darling Range Batholith, Western Australia. Contributions to Mineralogy and Petrology, 166(2), 511-523.

Pidgeon, R.T., Nemchin, A.A., and Whitehouse, M.J. (2017) The effect of weathering on U–Th–Pb and oxygen isotope systems of ancient zircons from the Jack Hills, Western Australia. Geochimica et Cosmochimica Acta, 197, 142-166.

Schmidt, C., and Nasdala, L. (2020) Applications of Raman Spectroscopy in Mineralogy and Geochemistry. Elements, 16(2), 99-104.

Trail, D., Thomas, J.B., and Watson, E.B. (2011) The incorporation of hydroxyl into zircon. American Mineralogist, 96(1), 60-67.

Valley, J.W., Chiarenzelli, J.R., and McLelland, J.M. (1994) Oxygen isotope geochemistry of zircon. Earth and Planetary Science Letters, 126(4), 187-206.

Wang, R., Jeon, H., and Evans, N.J. (2018) Archaean hydrothermal fluid modified zircons at Sunrise Dam and Kanowna Belle gold deposits, Western Australia: Implications for post-magmatic fluid activity and ore genesis. American Mineralogist, 103(12), 1891-1905.

Wang, X.L., Coble, M.A., Valley, J.W., Shu, X.J., Kitajima, K., Spicuzza, M.J., and Sun, T.

(2014) Influence of radiation damage on Late Jurassic zircon from southern China: Evidence from in situ measurements of oxygen isotopes, laser Raman, U–Pb ages, and trace elements. Chemical Geology, 389, 122-136.

White, L.T., and Ireland, T.R. (2012) High-uranium matrix effect in zircon and its implications for SHRIMP U–Pb age determinations. Chemical Geology, 306-307, 78-91.

Woodhead, J.A., Rossman, G.R., and Silver, L.T. (1991a) The metamictization of zircon: radiation dose-dependent structural characteristics. American Mineralogist, 76(1-2), 74-82.

Woodhead, J.A., Rossman, G.R., and Thomas, A.P. (1991b) Hydrous species in zircon. American Mineralogist, 76(9-10), 1533-1546.

Xia, X.P., Cui, Z.X., Li, W.C., Zhang, W.F., Yang, Q., Hui, H.J., and Lai, C.K. (2019) Zircon water content: reference material development and simultaneous measurement of oxygen isotopes by SIMS. Journal of Analytical Atomic Spectrometry, 34(6), 1088-1097.

Xia, X.P., Meng, J.T., Ma, L., Spencer, C.J., Cui, Z.X., Zhang, W.F., Yang, Q., and Zhang, L. (2021) Tracing magma water evolution by H_2O-in-zircon: A case study in the Gangdese batholith in Tibet. Lithos, 404-405.

Xu, J., Xia, X.P., Wang, Q., Spencer, C.J., Lai, C.K., Ma, J.L., Zhang, L., Cui, Z.X., Zhang, W.F., and Zhang, Y.Q. (2021) Pure sediment-derived granites in a subduction zone. GSA Bulletin.

525 Xu, Y., Tang, W., Hui, H., Rudnick, R.L., Shang, S., and Zhang, Z. (2019) Reconciling the
526 discrepancy between the dehydration rates in mantle olivine and pyroxene during
527 xenolith emplacement. Geochimica et Cosmochimica Acta, 267, 179-195.
528 Yang, C.M., Xu, Y.G., Xiao, X.P., Gao, Y.Y., Zhang, W.F., Yang, Y.N., Yang, Q., and Zhang, L.
529 (2022) Raman spectroscopy-based screening of zircon for reliable water content and
530 oxygen isotope measurements. American Mineralogist, in press.
531 Yao, J., Cawood, P.A., Zhao, G., Han, Y., Xia, X., Liu, Q., and Wang, P. (2021) Mariana-type
532 ophiolites constrain the establishment of modern plate tectonic regime during
533 Gondwana assembly. Nat Commun, 12(1), 4189.
534 Zhai, M.G., Guo, J.H., and Liu, W.J. (2005) Neoarchean to Paleoproterozoic continental
535 evolution and tectonic history of the North China Craton: a review. Journal of Asian
536 Earth Sciences, 24(5), 547-561.
537 Zhang, M., Salje, E.K.H., and Ewing, R.C. (2003) Oxidation state of uranium in metamict
538 and annealed zircon: near-infrared spectroscopic quantitative analysis. Journal of
539 Physics: Condensed Matter, 15(20), 3445-3470.
540 Zhang, M., Salje, E.K.H., and Ewing, R.C. (2010) OH species, U ions, and CO/CO_2 in
541 thermally annealed metamict zircon ($ZrSiO_4$). American Mineralogist, 95(11-12),
542 1717-1724.
543 Zhang, P.P. (2015) Hydrogen diffusion in NAMs: andradite garnet and zircon. Unité
544 Matériaux et Transformations, Doctor, p. 218. Université de Lille, Lille.
545

546 **Figure captions**

547 **Figure 1.** Cathodoluminescence images of Sz2 (upper) and THX13120 (lower) at different
548 thermal annealing conditions. Red circle represents SIMS analysis spots. The numbers below
549 each zircon grains are water content (left) and $\delta^{18}O$ (right). Most zircon grains are > 100 μm
550 long.

551

552 **Figure 2.** Water contents of zircons heated at different temperatures for 2 hours: (a) Penglai:
553 crystalline zircon. (b) Sz2: crystalline and coexisting highly-metamict zircons. (c) THX13120:
554 mostly metamict zircons. The Penglai and Sz2 zircon data at room temperature (RmT) are
555 from Yang et al. (2022), and the THX13120 data (RmT) are from Cui et al. (2022). All the
556 samples were placed inside a 50°C oven before SIMS analysis to avoid surficial water
557 adsorption from the air. The number of analysis spots are at the bottom of each panel.

558

559 **Figure 3.** $\delta^{18}O$ variation for the zircon Penglai (a), Sz2 (b), and THX13120 (c) at different
560 temperatures for 2 hours. At >700°C, the $\delta^{18}O$ variation for Sz2 becomes more limited.

561

562 **Figure 4.** The water content in three zircon samples: Penglai (a), Sz2 (b), and THX13120 (c),
563 heated at 600°C for different time. The data at room temperature are the same as in Figure 2.
564 Note that the water contents of Penglai and THX13120 do not change with annealing time.
565 There is minor secondary water diffusion in Sz2 annealed for less than 4 hours, and massive
566 diffusion when annealed for over 6 hours.

567

568 **Figure 5.** The $\delta^{18}O$ of three zircon samples annealed at 600℃ for different time: Penglai (a),
569 Sz2 (b), and THX13120 (c),

570

571 **Figure 6.** Comparison of Raman spectrum of zircon Sz2 (a) and THX13120 (b) annealed at
572 different temperatures. Labels on the right represents the annealing temperature (upper, ℃)
573 and time (lower, hour). The metamict zircon is distinct from crystalline zircon by its smooth
574 spectrum. The spectra are displayed with different colors for clarity. Highly metamict zircons
575 in Sz2 are still present when heated at 400℃, but disappeared at 800℃ and 1000℃. Most
576 untreated zircons (at RmT) of THX13120 are metamict. Some metamict zircons are healed at
577 600℃, and most become crystalline at 1000℃.

578

579 **Figure 7.** Plots of water content versus $\delta^{18}O$ of Sz2 (a) and THX13120 (b). The zircons
580 unannealed or annealed at <600℃ for 2 hours are denoted by green triangles. They preserved
581 their secondary waters from thermal diffusion. The zircon grains that were annealed at 600℃
582 for >4 hours are marked with red circles, in which the secondary water was effectively
583 removed. Error bars indicate 2σ errors; (c-d) Discrimination plots of magmatic and
584 hydrothermal zircons. $(Sm/La)_N$ is chondrite-normalized (Hoskin et al., 2005), whilst LREE-I
585 (LREE index) is defined by (Dy/Nd)+(Dy/Sm) (Bell et al., 2016).

586

This is the peer-reviewed, final accepted version for American Mineralogist, published by the Mineralogical Society of America.
The published version is subject to change. Cite as Authors (Year) Title. American Mineralogist, in press.
DOI: https://doi.org/10.2138/am-2022-8444. http://www.minsocam.org/

587 **Figure 8.** Calculated ratio of annealed zircon water content to its initial water content,
588 according to Xu et al. (2019). The zircons with 100 μm diameter are assumed to be heated at
589 600–1000°C for 2 hours (see text for details).

590

591 **Figure 9.** Water content (a) and $\delta^{18}O$ (b) of three zircon groups from Sz2. The
592 Raman-screened crystalline zircons preserve primary geochemical signature. The zircons
593 annealed at 600°C for >4 hours likely retrieve the primary water contents but expel all
594 secondary water. By contrast, heating at >700°C for 2 hours likely removed both primary and
595 secondary waters.

596

This is the peer-reviewed, final accepted version for American Mineralogist, published by the Mineralogical Society of America.
The published version is subject to change. Cite as Authors (Year) Title. American Mineralogist, in press.
DOI: https://doi.org/10.2138/am-2022-8444. http://www.minsocam.org/

Figure 1

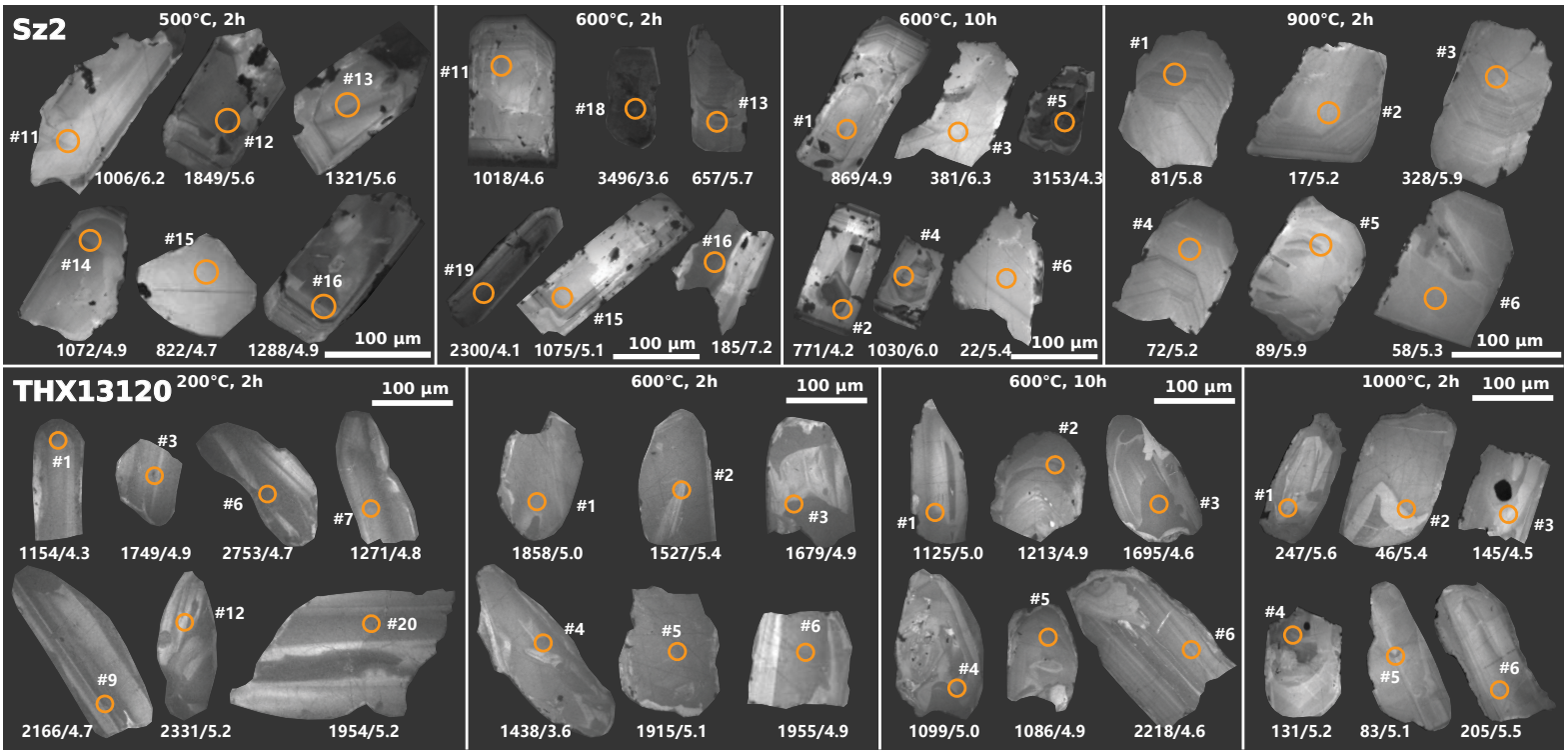

This is the peer-reviewed, final accepted version for American Mineralogist, published by the Mineralogical Society of America.
The published version is subject to change. Cite as Authors (Year) Title. American Mineralogist, in press.
DOI: https://doi.org/10.2138/am-2022-8444. http://www.minsocam.org/

Figure 2

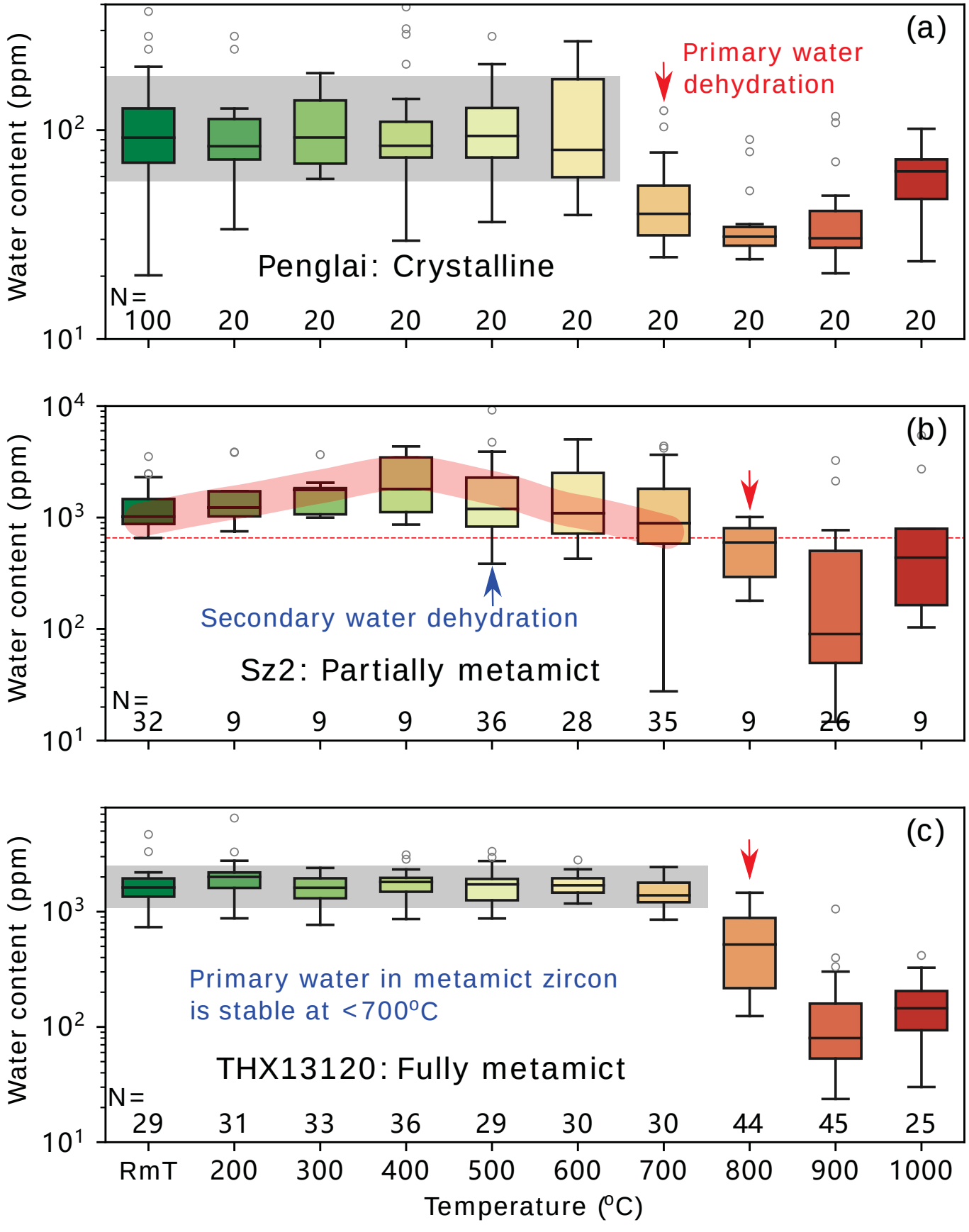

This is the peer-reviewed, final accepted version for American Mineralogist, published by the Mineralogical Society of America.
The published version is subject to change. Cite as Authors (Year) Title. American Mineralogist, in press.
DOI: https://doi.org/10.2138/am-2022-8444. http://www.minsocam.org/

Figure 3

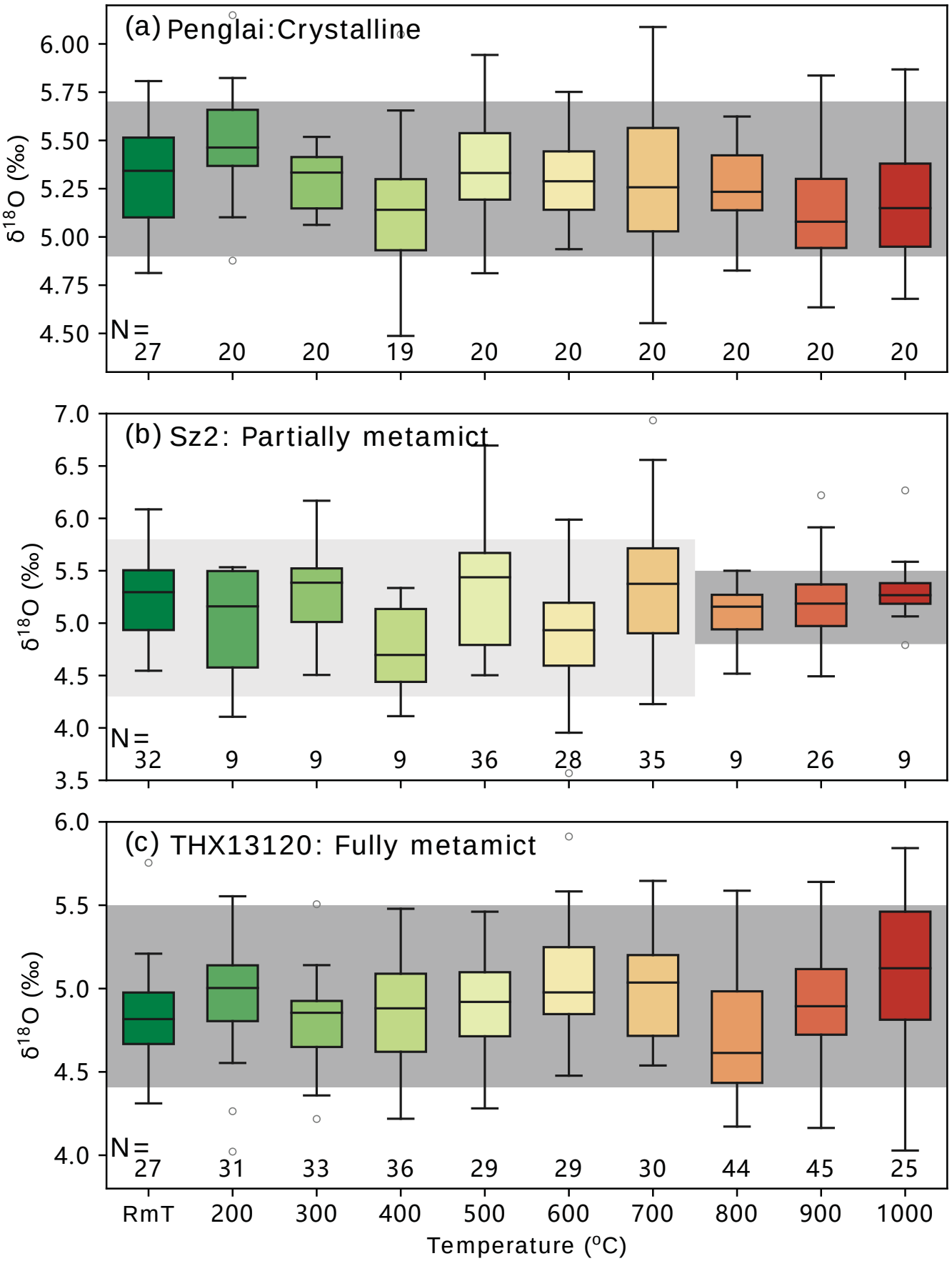

This is the peer-reviewed, final accepted version for American Mineralogist, published by the Mineralogical Society of America.
The published version is subject to change. Cite as Authors (Year) Title. American Mineralogist, in press.
DOI: https://doi.org/10.2138/am-2022-8444. http://www.minsocam.org/

Figure 4

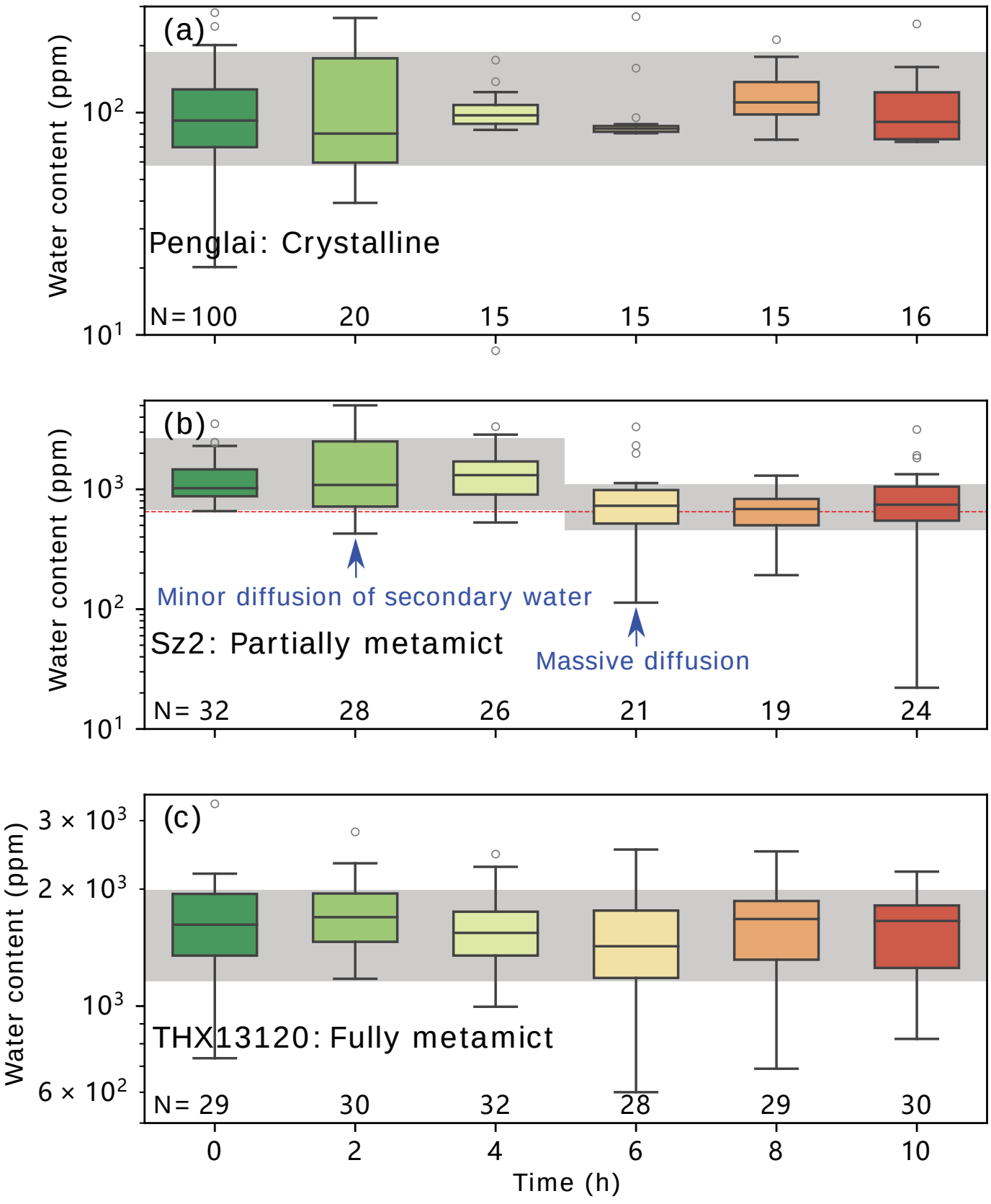

This is the peer-reviewed, final accepted version for American Mineralogist, published by the Mineralogical Society of America.
The published version is subject to change. Cite as Authors (Year) Title. American Mineralogist, in press.
DOI: https://doi.org/10.2138/am-2022-8444. http://www.minsocam.org/

Figure 5

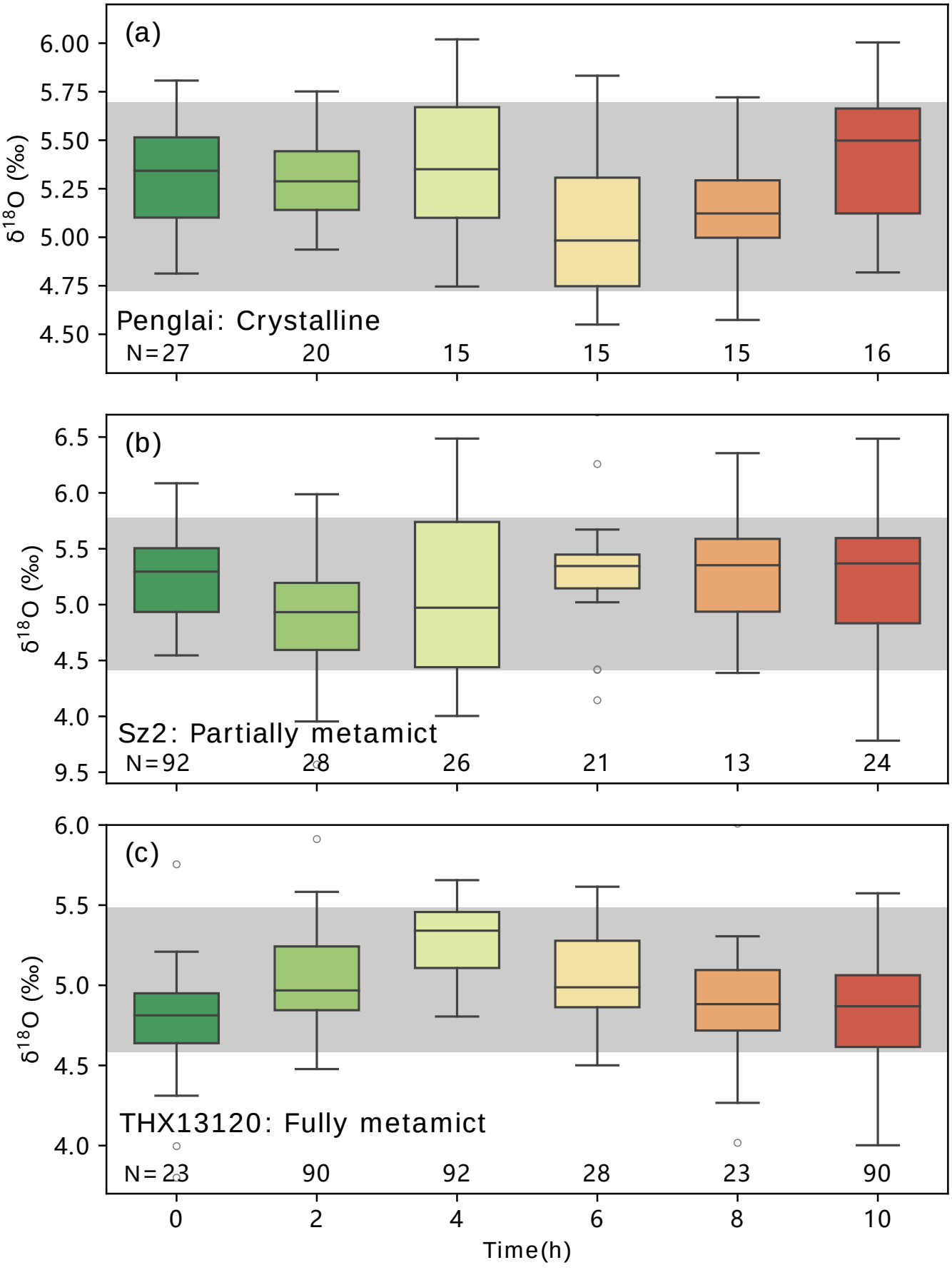

This is the peer-reviewed, final accepted version for American Mineralogist, published by the Mineralogical Society of America.
The published version is subject to change. Cite as Authors (Year) Title. American Mineralogist, in press.
DOI: https://doi.org/10.2138/am-2022-8444. http://www.minsocam.org/

Figure 6

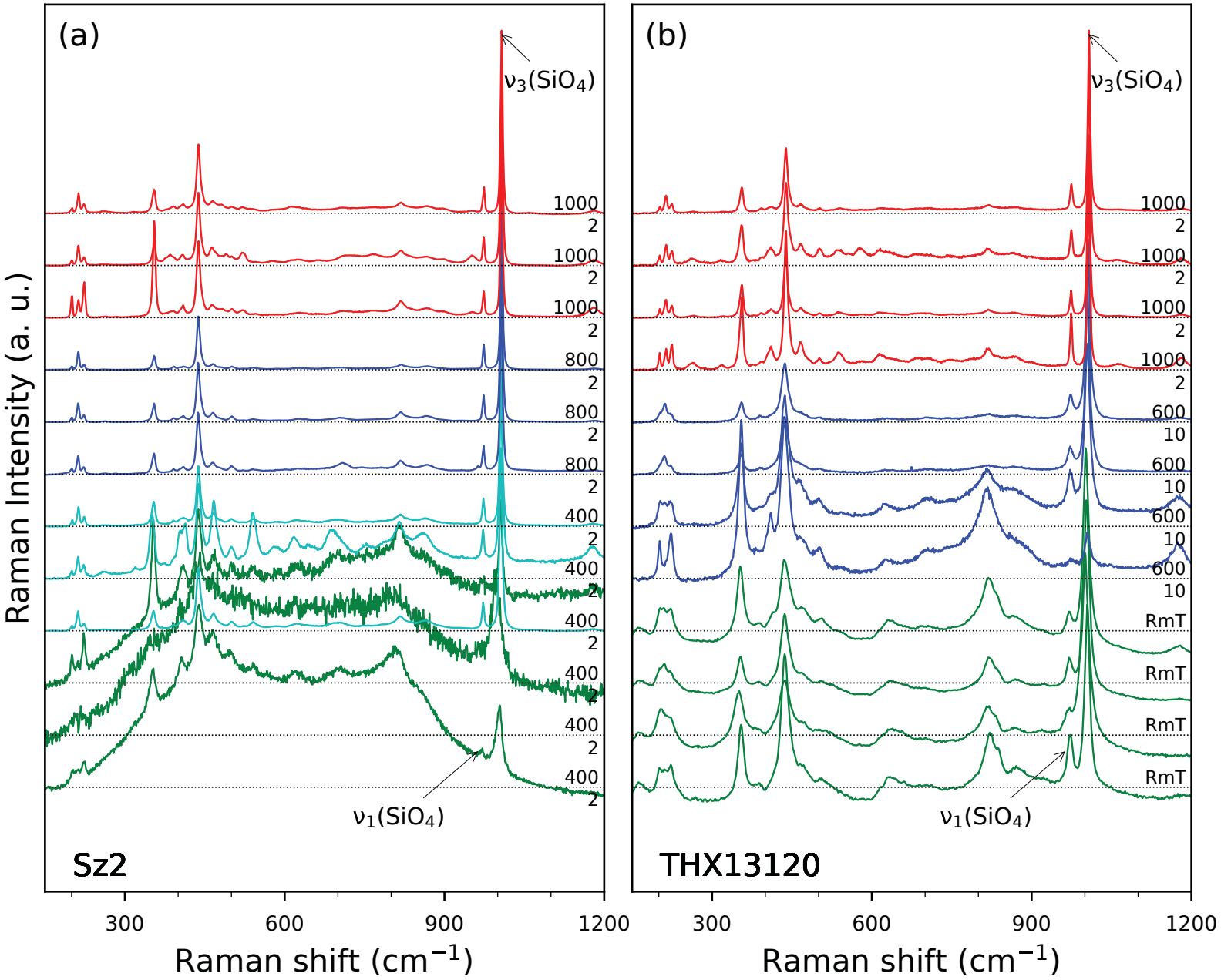

This is the peer-reviewed, final accepted version for American Mineralogist, published by the Mineralogical Society of America.
The published version is subject to change. Cite as Authors (Year) Title. American Mineralogist, in press.
DOI: https://doi.org/10.2138/am-2022-8444. http://www.minsocam.org/

Figure 7

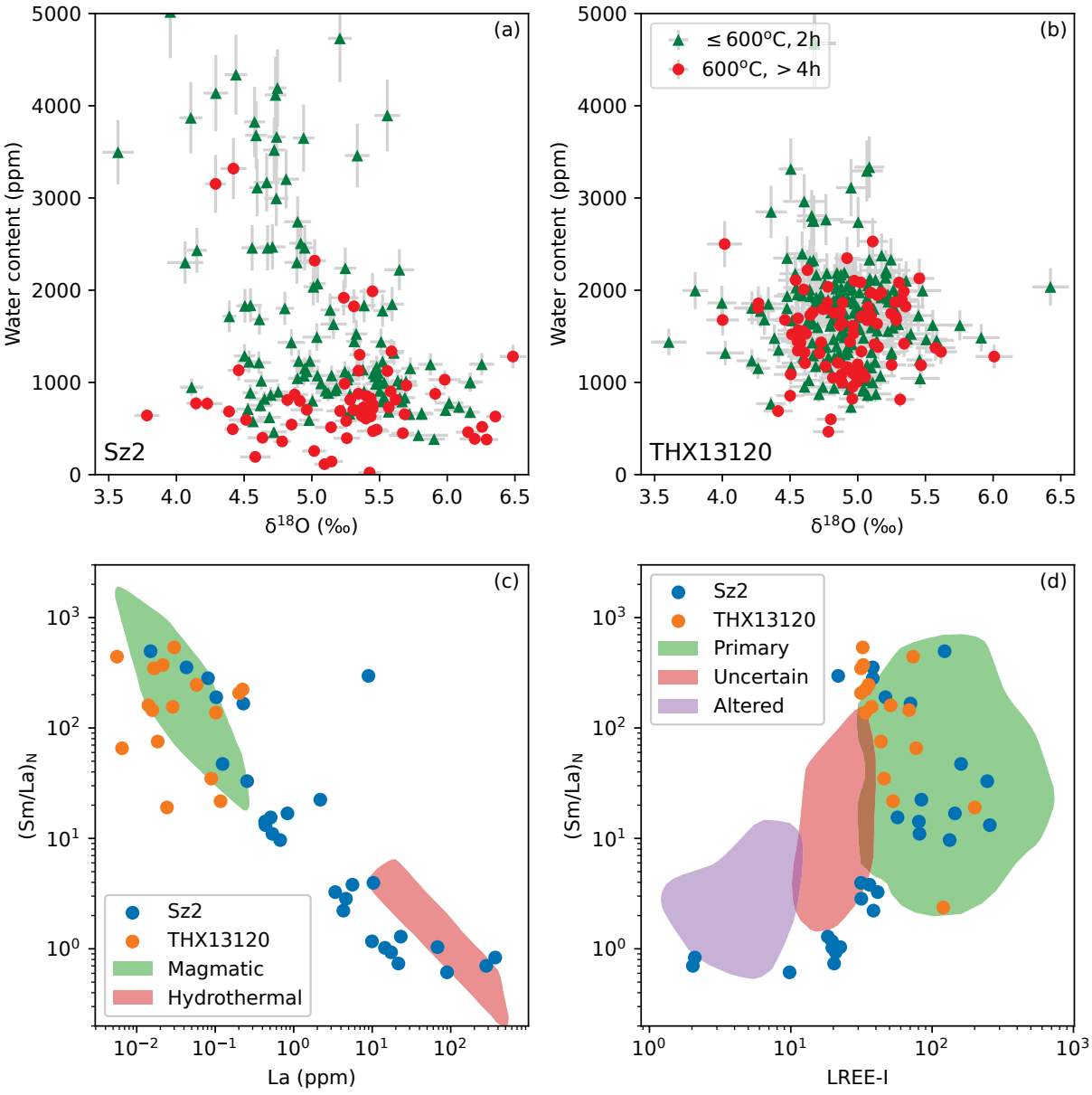

This is the peer-reviewed, final accepted version for American Mineralogist, published by the Mineralogical Society of America.
The published version is subject to change. Cite as Authors (Year) Title. American Mineralogist, in press.
DOI: https://doi.org/10.2138/am-2022-8444. http://www.minsocam.org/

Figure 8

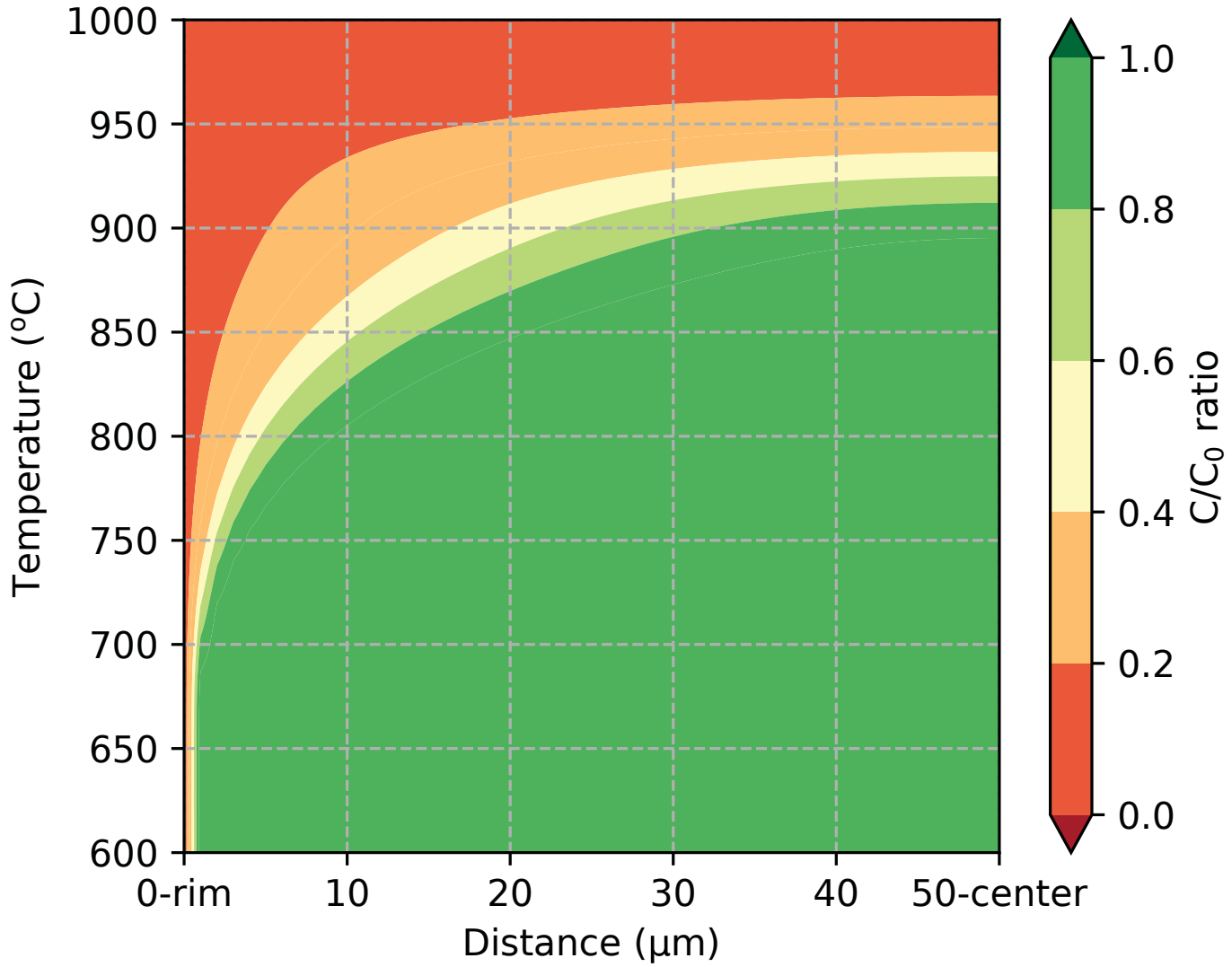

This is the peer-reviewed, final accepted version for American Mineralogist, published by the Mineralogical Society of America.
The published version is subject to change. Cite as Authors (Year) Title. American Mineralogist, in press.
DOI: https://doi.org/10.2138/am-2022-8444. http://www.minsocam.org/

Figure 9